

A Study of the Catalytic Oxidation of Benzene to Maleic Anhydride

BASIL DMUCHOVSKY, MARSHALL C. FREERKS, EMILE D. PIERRON,
RALPH H. MUNCH, AND FERDINAND B. ZIENTY

*From the Advanced Organic Chemicals Research Laboratory, Organic Chemicals Division,
Monsanto Company, St. Louis, Missouri*

Received July 31, 1964; revised September 14, 1964

Rate data are presented for the catalytic oxidation of benzene to maleic anhydride, CO and CO₂ on a vanadia-molybdena catalyst. The catalyst is well defined by physical and chemical analysis including X-ray diffraction studies, titration of vanadium, EPR examination, surface area, and pore volume. A first order rate law is obeyed over the first 75% of reaction for several temperatures in the range 319° to 377°C. It is concluded that benzene is oxidized in two independent ways, one path leading to oxides of carbon and the other to maleic anhydride, which is further oxidized. First order rate constants and apparent activation energies are given for the three paths. A partial mechanism accounting for the results is suggested by the use of absolute rate theory. It is proposed that in the rate-limiting step benzene can add molecular oxygen either in a 1,2- or 1,4- fashion to yield activated complexes possessing considerable mobility.

INTRODUCTION

Despite numerous references to the catalytic oxidation of benzene to maleic anhydride (1) few detailed mechanisms have been proposed to account for the course of the reaction. Kinetic investigations reveal that the over-all reaction sequence can be represented adequately by two competitive pathways for benzene consumption, one of which leads to complete oxidation and the other to maleic anhydride which can be further oxidized. The three kinetic steps are considered to be uninhibited first order reactions with equal apparent activation energies. More recent reports show disagreement with the older data. Butler and Weston (2) assume that the oxidation of maleic anhydride is negligible up to 20% consumption of benzene and Ioffe and Lyubarskii (3) demonstrate that the rate of reaction is inhibited by maleic anhydride and that the three steps have unequal activation energies.

The available evidence suggests that the reaction must start and finish at the same surface site with no migration of intermediates (1a). It is postulated that hydrocarbon

is adsorbed with the abstraction of hydrogen (4) to form a radical which combines with oxygen striking it from the vapor phase. Further reaction is thought to proceed through the formation and destruction of surface peroxy radicals.

The role of the catalyst in the reaction is still not clear but EPR studies demonstrate the existence of unpaired electrons in the bulk of vanadia-molybdena catalysts (5-7). A study of partially reduced vanadium pentoxide identifies paramagnetic species as being associated with the vanadium and not with oxygen (8). Stable paramagnetic surface species derived from naphthalene and anthracene have been observed on vanadium pentoxide (9); the introduction of air increases the signal intensity of the adsorbed species and causes a corresponding signal even in the case of benzene, which indicates that benzene alone does not form a stable surface species. These results suggest that interaction between the reactants and the catalyst takes place through the agency of an unpaired electron. This is borne out by the work of Ioffe and co-workers (7) who

demonstrated that the activity of vanadia-molybdena catalysts is directly proportional to the intensity of the EPR signal which also is related in a complex way to the amount of molybdena in the mixed catalyst.

The source of the oxygen used is a matter of dispute. In the absence of air in a closed system V_2O_5 can function as a reagent to supply lattice oxygen to a hydrocarbon (10). Some workers (1, 3, 11) have proposed that in a flow system the V_2O_5 catalyst is reduced by supplying lattice oxygen to the adsorbed species and is then reoxidized by atmospheric oxygen. In addition to the oxidation of benzene by adsorbed oxygen (2), Ioffe and Lyubarskii (3) claim that the oxidation of strongly adsorbed maleic anhydride uses lattice oxygen. However, recent work by Roiter and Yuza (12) reveals that the oxidation of hydrogen on V_2O_5 is considerably faster than catalyst oxidation or reduction and confirms earlier work using O^{18} (13). Bond (14) generalizes that covalent metal oxides (as is the vanadia-molybdena system) do not readily gain or lose oxygen whereas oxygen is fairly readily removed from or added to ionic oxides. Nevertheless, even with ionic oxides the oxidation of CO largely uses atmospheric oxygen (15). The tendency to use vapor phase rather than lattice oxygen should thus be enhanced with covalent oxides. This deduction is supported by work showing that the activation energy for O^{18} exchange with a V_2O_5 catalyst (13, 16) is greater than the activation energy for benzene oxidation (2) and naphthalene oxidation (17). Further support is furnished by the fact that oxygen is readily and reversibly adsorbed on V_2O_5 surfaces (18-21).

The present study is an attempt to develop greater insight into the interactions among the reactants and a vanadia-molybdena catalyst in a catalytic oxidation of benzene.

RESULTS AND TREATMENT OF DATA

Since these experiments were carried out with an initial oxygen-to-benzene ratio of about 16 (ca. 1.3% by volume benzene in air) any variation in oxygen partial pressure would be small so it is assumed that the rate of reaction is independent of the oxygen

concentration; this is supported by the work of Ioffe and Lyubarskii (3) and that of Hayashi and co-workers (22). This is further substantiated by a few experiments using 10% O_2 in air which were indistinguishable from runs using normal air.

The reasonably good fit of the rate of benzene disappearance to a simple first order expression is shown in Fig. 1, where $[B]_0$ is

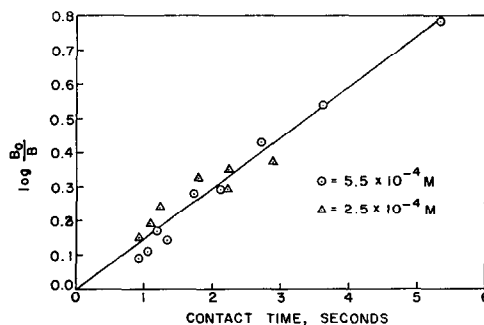
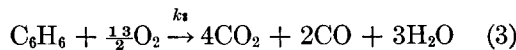
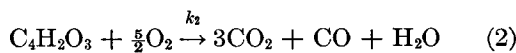
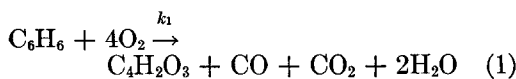


FIG. 1. First order plot of benzene disappearance at 343° at two different initial concentrations of benzene.

the initial concentration of benzene and $[B]$ is the concentration at time t for two different initial concentrations of benzene. The linear relationship holds to 85% reaction and indicates that the rate is not sensibly affected by the products of reaction in the integral reactor flow system up to this extent of reaction. Data for reaction at 357°C show that about 5 moles of oxygen are required for each mole of benzene consumed; therefore, the ratio of oxygen to benzene remaining will increase with conversion and will maintain the zero order in oxygen throughout the course of reaction. It is assumed that the rates of carbon oxide and maleic anhydride (MA) formation are simple pseudo-first-order reactions. The treatment ignores the negligible volume increase.

The following kinetic model for the reaction sequence is chosen and is similar to that used by other investigators (1, 3). The rate expressions can be solved in closed form and are shown using the symbols B for benzene and MA for maleic anhydride with concentration units of moles per liter at STP.



$$-d[\text{B}]/dt = (k_1 + k_3)[\text{B}] \quad (4)$$

$$d[\text{MA}]/dt = k_1[\text{B}] - k_2[\text{MA}] \quad (5)$$

$$d[\text{CO}]/dt = (k_1 + 2k_3)[\text{B}] + k_2[\text{MA}] \quad (6)$$

$$d[\text{CO}_2]/dt = (k_1 + 4k_3)[\text{B}] + 3k_2[\text{MA}] \quad (7)$$

$$[\text{B}] = [\text{B}]_0 \exp - (k_1 + k_3)t = [\text{B}]_0 e^{-k_B t} \quad (8)$$

$$[\text{MA}] = \frac{k_1[\text{B}]_0}{k_2 - (k_1 + k_3)} \frac{1}{\exp - (k_1 + k_3)t - \exp (-k_2 t)} \quad (9)$$

$$= \frac{k_1[\text{B}]_0}{k_2 - k_B} [e^{-k_B t} - e^{-k_2 t}]$$

$$[\text{CO}] = \frac{[\text{B}]_0}{k_1 - k_3} \left[-k_1 - 2k_3 - \frac{k_1 k_2}{k_2 - k_B} \right] [e^{-k_B t} - 1] + \frac{k_1[\text{B}]_0}{k_2 - k_B} [e^{-k_2 t} - 1] \quad (10)$$

$$[\text{CO}_2] = \frac{[\text{B}]_0}{k_1 + k_3} \left[-k_1 - 4k_3 - \frac{3k_1 k_2}{k_2 - k_B} \right] [e^{-k_B t} - 1] + \frac{3k_1[\text{B}]_0}{k_2 - k_B} [e^{-k_2 t} - 1] \quad (11)$$

The value of $k_1 + k_3$ is found from the use of the raw data for the disappearance of benzene as shown by the representative data in Table 1 and Eq. (8). Equation (9) then is recast into more convenient form by multiplying through both sides of the equation

TABLE 1
RATE DATA FOR BENZENE OXIDATION AT 331°C

| Time (sec) | $[\text{B}]_0^a$ | $[\text{B}]_t$ | $[\text{CO}]$ | $[\text{CO}_2]$ | $[\text{MA}]$ |
|------------|------------------|----------------|---------------|-----------------|---------------|
| 0.92 | 5.45 | 4.86 | 0.99 | 1.62 | 0.23 |
| 1.12 | 5.38 | 4.29 | 1.78 | 2.84 | 0.49 |
| 1.71 | 5.33 | 3.85 | 2.21 | 3.87 | 0.72 |
| 2.70 | 5.22 | 2.82 | 3.60 | 6.30 | 1.13 |
| 3.63 | 5.42 | 2.23 | 4.86 | 8.28 | 1.52 |
| 5.18 | 5.42 | 1.69 | 5.63 | 9.50 | 1.54 |

^a Concentration, 10^{-4} moles/liter, STP.

by $1/[\text{B}]_0[\exp - (k_1 + k_3)t - \exp (-k_2 t)]$. The use of the experimental molar ratios $[\text{MA}]/[\text{B}]_0$ at two contact times together with the experimentally determined constant, $k_1 + k_3$, allows a value for k_2 to be found. It then is a simple task to compute k_1 and k_3 individually. Table 2 lists the Arrhenius parameters found by this method for the temperature range 319° to 377°C.

TABLE 2
VALUES OF THE ARRHENIUS PARAMETERS

| | $\log A$ (sec^{-1}) | E_a (kcal/mole) |
|-------|-----------------------------------|----------------------|
| k_1 | 11.7 | 35 ± 2 |
| k_2 | 0.4 | 4.9 ± 0.5 |
| k_3 | 8.4 | 26 ± 2 |

The stoichiometry of each step in the assumed kinetic model [Eqs. (1), (2) and (3)] allows the best reproduction of the data over the entire range of experimentation. The close agreement between the calculated and observed concentration ratios is illustrated in Fig. 2 and Fig. 3 and is shown in

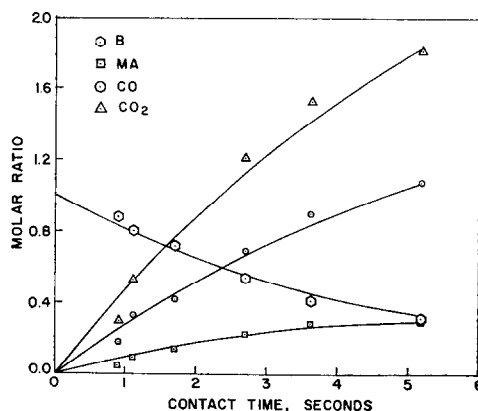


FIG. 2. Comparison of observed and calculated molar ratios of products to initial concentration of benzene as a function of time at 331°. The points are experimental values.

Table 3 for reaction at 357°. The latter table reveals that the $[\text{MA}]/[\text{B}]_0$ ratio reaches a maximum and decreases with increasing time, thereby confirming the consecutive reaction scheme adopted.

Figure 4 shows the comparison between

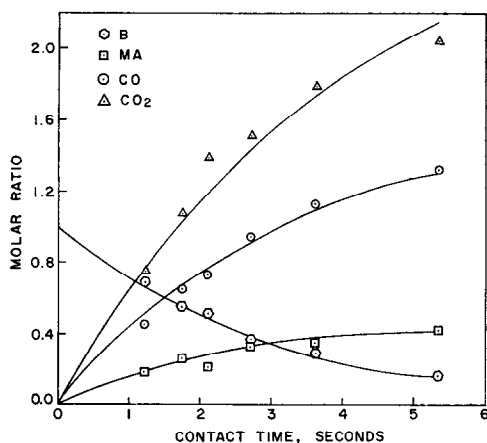


FIG. 3. Comparison of observed and calculated molar ratios at 343°C.

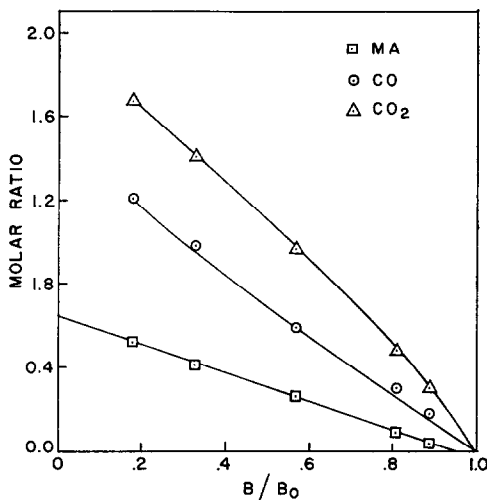


FIG. 4. Comparison of observed and calculated ratios at 0.93 sec and changing temperature (varying [B] reaction). The points are experimental values.

the calculated and observed ratios of [B], [CO], [CO₂], and [MA] for data taken at a constant time of 0.93 sec and changing temperature between 319° and 377°C. Figure 5 shows that $[MA]/([B]_0 - [B])$, the ratio of [MA] found to benzene reacted, increases with increasing temperature at a constant time of 0.93 sec. This finding supports the assignment of the highest apparent activation energy in the reaction sequence to step (1), the formation of maleic anhydride.

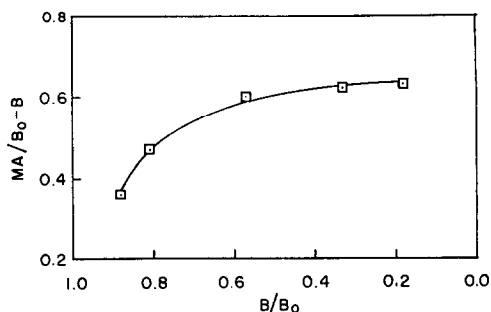


FIG. 5. The ratio of [MA] to [B] reacted at 0.93 sec and changing temperature.

The time required for the maximum molar ratio, $[MA]/[B]_0$, at a given temperature, can be found by differentiating Eq. (9) with respect to time, setting the result equal to zero and solving for t (23).

$$t_{\max} = \frac{1}{k_2 - (k_1 + k_3)} \ln \frac{k_1}{k_1 + k_3} \quad (12)$$

Substituting a value for t_{\max} (found by plotting the data in Table 3) and $k_1 + k_3$ into Eq. (12) leads to a value for k_2 that is the same as that found by the method outlined previously.

TABLE 3
COMPARISON OF CALCULATED AND OBSERVED
MOLAR RATIOS AT 357°C

| Time (sec) | [B]/[B] ₀ obs | [B]/[B] ₀ calc | [MA]/[B] ₀ obs | [MA]/[B] ₀ calc |
|------------|-----------------------------|------------------------------|------------------------------|-------------------------------|
| 0.94 | 0.57 | 0.56 | 0.26 | 0.27 |
| 1.07 | 0.50 | 0.52 | 0.30 | 0.28 |
| 1.24 | 0.43 | 0.47 | 0.34 | 0.31 |
| 1.46 | 0.41 | 0.41 | 0.34 | 0.34 |
| 1.74 | 0.35 | 0.34 | 0.38 | 0.38 |
| 2.73 | 0.21 | 0.19 | 0.43 | 0.44 |
| 5.36 | 0.10 | 0.04 | 0.42 | 0.43 |

The close agreement between the calculated and observed molar ratios indicates that the proposed reaction sequence, rate constants, and stoichiometries are consistent with all the experimental observations.

Our EPR study shows that unpaired electrons do exist in the vanadia-molybdena system, although it was not possible to determine which metal atom bears the unpaired electron.

The influence of pore diffusion on the observed kinetics is estimated by using the equations and criteria developed by Wheeler (24) and by Weisz and Prater (25). The values used are 0.4 cm pellet radius, 1.66 m²/g surface area, 0.96 g/cm³ catalyst density, 5.4×10^{-7} moles/cm³ reactant concentration, 1.3×10^{-7} moles/m² sec specific rate, 0.15 cm³/g pore volume and 0.27 cm²/sec estimated diffusivity value (26). The ratio of the observed rate constant to the diffusion rate constant is less than one, which satisfies Wheeler's conditions and suggests that all of the internal surface area of the catalyst is available for reaction. Weisz and Prater's conditions of particle size and diffusivity for which no diffusion effects occur also are satisfied. In the absence of experimental measured diffusivities and the influence of particle size, these calculations are only suggestive at best. However, even if diffusion effects were important, the ratio of rate constants k_1/k_3 will not be affected. It is concluded that the observed kinetics are those of a surface reaction, particularly in view of the relatively high activation energy and the linear relationship between $\ln k$ and $1/T$ over a 59° temperature range.

Halving the weight of the catalyst at constant flow rate decreases the rate twofold, thus demonstrating that the rate is directly proportional to the catalyst weight and hence the surface area.

DISCUSSION

One of the more interesting and hitherto unanswered questions raised by this and previous studies is why benzene reacts by two different paths. In order to attempt an answer it is necessary to focus attention on the step in the reaction sequence where the divergence occurs. It is assumed that the rate-limiting step for both paths is the same. That the respective activated complexes must differ is attested to by the different activation energies found. The problem is reduced to ascertaining the rate-limiting step for the disappearance of benzene by the use of the theory of absolute reaction rates (27). The assumptions inherent in the appli-

cation of absolute rate theory to heterogeneous reactions are understood to apply (28).

The rate of benzene consumption is first order in benzene, independent of oxygen under the reaction conditions employed, and proportional to the weight of catalyst. These observations indicate that the surface is saturated with atomic and/or molecular oxygen and further suggest that the slow step is the reaction of benzene with the film of oxygen species covering the surface. The appropriate equation describing the disappearance of benzene in molecules per second per cm² of surface is

$$v = c_B c_a (kT/h) (f_{\ddagger}/F_B F_a) e^{-E_0/RT} \quad (13)$$

where c_B is the concentration of benzene in the gas phase, initially 3.3×10^{-17} molecules per cc (STP) and c_a is the concentration of surface oxygen species. With the assumption that molecular oxygen is the dominant surface species, having a molecular area of 20 Å², c_a becomes 5×10^{14} molecules/cm²; c_a increases by a factor of 2 if atomic oxygen is chosen. F_B is the partition function of benzene at unit concentration and is 6.5×10^{32} at 630°K. F_a and f_{\ddagger} are the partition functions for adsorbed oxygen and the activated complex, respectively, and the other terms have their usual meanings.

Substitution of these values into Eq. (13) for 630°K leads to

$$v_1 = 2.9 (f_{\ddagger}/F_a) \quad (14)$$

for path (1) (leading to maleic anhydride) with an apparent activation energy of 35 kcal/mole and for path (3), having an activation energy of 26 kcal/mole, the expression is

$$v_3 = 3.6 \times 10^3 (f_{\ddagger}/F_a) \quad (15)$$

The observed rates at this temperature are 5.0×10^{12} for v_1 and 3.0×10^{12} for v_3 , in molecules per second per cm² of surface. It is clear that the ratio f_{\ddagger}/F_a must be 10^9 to 10^{12} in order to satisfy the experimental results. This implies that the activated complex must have substantially more freedom than the adsorbed oxygen. Consequently, the entropy of activation should be less than that anticipated for complete loss of the translational and rotational freedom

of benzene. The experimental standard entropy of activation, ΔS_e^\ddagger , is -95 gibbs/mole for path (1) and -110 gibbs/mole for path (3), the standard state being unit concentration. The expected value for the loss of all translational (128 gibbs/mole) freedom and all rotational (21 gibbs/mole) freedom is -149 gibbs/mole. The difference of 54 gibbs/mole for path (1) is the entropy of the activated complex in excess of that possessed by the adsorbed oxygen. This value can then be used to calculate the ratio f_\ddagger/F_a to be 6.3×10^{11} for path (1) and 3.3×10^8 for path (3). The calculated rates are $v_1 = 1.8 \times 10^{12}$ and $v_3 = 1.2 \times 10^{12}$ molecules/sec/cm² in satisfactory agreement with experiment.

If the adsorbed oxygen is immobile then F_a is 1 and the activated complex has one translational degree of freedom, probably normal to the surface. If the adsorbed oxygen has one degree of translational freedom or its equivalent (as two hindered translations) then the activated complex is a two-dimensional gas. The latter situation for adsorbed oxygen is precisely that envisaged for the adsorption of nitrogen on doubly-promoted iron (29) and is plausible in view of the recent experiments demonstrating the mobility of oxygen on platinum (30) and the ready, reversible adsorption of oxygen on vanadium oxide (18-21). In either case, however, there is rather striking mobility of the activated complex.

There is ample evidence for the mobility of physically adsorbed benzene on mercury (31), alumina (32), magnesium oxide, nickel oxide, and zinc oxide (33). In all cases the experimental entropy of adsorption agreed with that calculated for the model of benzene adsorbed parallel to the surface and having two degrees of translational freedom and rotation in the plane of the ring. On the basis of such evidence one cannot distinguish between gas-phase benzene attacking the surface in the rate-limiting step or the reaction between two-dimensional benzene and adsorbed oxygen.

The explanation for the existence of two paths in the reaction of benzene must reside in the manner in which the attack on oxygen occurs. One can visualize either 1,2 addition

leading to activated complex (A) or 1,4 addition giving activated complex (B). This is the same kind of attack proposed by



Boocock and Cvetanovic (34) for the reaction of oxygen atoms with benzene. The subscript x is either 1 or 2 depending upon the number of oxygen atoms involved. Structure (A) should be of lower energy because of the resonance energy of the conjugated system which is 3 or 3.5 kcal/mole (35). We can, therefore, identify structure (B) resulting from 1,4 addition with the higher energy path leading to maleic anhydride and structure (A) with the path resulting in complete oxidation.

The difference in the entropies of activation for the two paths, $\Delta\Delta S_e^\ddagger$, is 15 gibbs/mole which corresponds to rotational differences. Either there are two kinds of adsorbed oxygen involved or the activated complexes differ in mobility.

The nature of the products formed from the catalytic oxidation of benzene is vastly different from that found in the vapor-phase reaction of benzene with oxygen atoms (34). This suggests that the catalyst plays a critical role, albeit unknown at the present time, in controlling the direction of the reaction. These facts also imply that atomic oxygen is not important in the catalytic reaction and that the reaction is completed at the surface.

Several other interesting points should be noted. Why should the addition of oxygen to benzene require about 30 kcal/mole at a surface when the addition of oxygen atoms in the vapor phase demands only 5 kcal/mole? Why are the apparent activation energies for the catalytic oxidations of naphthalene (1, 17, 36), toluene (1, 37), and benzene on vanadia-based catalysts all about 29 kcal/mole? Why should the activity of these catalysts be proportional to the number of unpaired electrons (?). In the interest of stimulating research we submit that the answer to the foregoing questions may well involve electronically excited molecular oxygen adsorbed on the surface.

Excitation of oxygen from the triplet ground state to a singlet state takes 23 kcal/mole (38) and can be induced by the mixed metal oxide, which has unpaired electrons, in the same way that the promotion of benzene to the triplet state is assisted by the presence of oxygen (39). The apparent activation energy which is necessary for the reactants to reach the transition state is the sum of the excitation energy and that needed for the act of addition. This figure is 28 kcal/mole if 5 kcal/mole is selected, after Boocock and Cvetanovic (34), for addition and is in satisfactory agreement with experiment.

In summary, the partial mechanism advanced accounts for the absolute rate of benzene disappearance, the fact that two paths exist, and the energy difference between the alternate routes.

EXPERIMENTAL

Catalyst preparation (40). Acid-washed carborundum pellets (340 g) were impregnated with a solution of 48.6 g of NH_4VO_3 , 24 g of $(\text{NH}_4)_6\text{Mo}_7\text{O}_{24}$, 2.76 g of $\text{Na}_3\text{PO}_4 \cdot 12\text{H}_2\text{O}$, and 2.12 g of $\text{Ni}(\text{NO}_3)_2 \cdot 6\text{H}_2\text{O}$ in 292 ml of concentrated hydrochloric acid. The mixture was concentrated in a porcelain casserole at steam bath temperature. The coated pellets were transferred to petri dishes and fired in air at 400°C for 52 min. The dark green, glossy coating comprised 14% by weight of the finished pellets, and completely covered the support.

Catalyst characterization. The ratio of V (IV) to total vanadium was found by a permanganate-ferrous sulfate titration method (41). The percentage of reduced vanadium in the coating solution was 34.4%, in the dry uncalcined pellet, 47.9%, and in the calcined pellet, 20.0%.

An Aminco-Winslow porosimeter (American Instrument Co., model No. 5-7108, Silver Spring, Md.) was used to determine that the surface area of the coated pellet was 1.66 m²/g and that the pore volume was 0.15 ml/g.

Electron paramagnetic resonance (EPR) measurements were made on a catalyst sample that was crushed and sieved to 100

mesh. The specimen was placed in a quartz sample tube and a room temperature probe was used in conjunction with a Varian EPR Spectrometer, Model V4500, operated with 100 kc modulation at a frequency of 9500 megacycles/sec. The anticipated signal was found, indicating the presence of unpaired electrons, in agreement with the literature (5-7) and the reduction found in the catalyst.

The composite catalyst was examined by X-ray powder diffraction methods. Since the interpretation of the data was hindered by the fact that the active coating was only 15% of the total catalyst, a duplicate preparation was made without the support. The *d* spacings of the active material in the supported and unsupported samples agreed exactly; however, more were observable for the coating alone. The diffraction pattern of the coating was compared with those of the synthetic compound oxides of vanadium and molybdenum described by Munch and Pierron (42). It was found that the X-ray diffraction pattern of the coating could be accounted for on the basis that its major components were the two compound oxides they describe. Both of these contain vanadium and molybdenum in the ratio 3/2 but differ in their oxygen content, the first having the empirical formula $\text{Mo}_6\text{V}_9\text{O}_{40}$ corresponding to 1/9 the vanadium in the V⁴⁺ state and the second $\text{Mo}_4\text{V}_6\text{O}_{25}$ to 2/3 the vanadium in the V⁴⁺ state. The X-ray diffraction data for the catalyst coating is given along with those for the two compound oxides in Table 4. Our experience shows that the X-ray diffraction pattern of the coating does not change after use under the reaction conditions described below.

Materials. Compressed air supplied by the National Cylinder Gas Company was used as received. Thiophene-free benzene (C.P. grade) was obtained from the Fisher Scientific Company.

Analyses. The benzene concentrations in the feed and product streams were determined by continual UV absorption spectroscopy using a Model 3 Micromatic Photoelectric Analyzer. An MSA IR analyzer, Model 200, was used to monitor the concentration of CO₂ produced by the reaction.

TABLE 4
 X-RAY POWDER DIFFRACTION PATTERNS^a

| Catalyst coating | Vanadium molybdenum oxides | | | | |
|------------------|---|-----------------|--|-----------------|----------------------------------|
| | Mo ₆ V ₂ O ₈ | | Mo ₄ V ₆ O ₂₈ | | |
| <i>d</i> (Å) | <i>I</i> / <i>I</i> ₁ ^b | <i>d</i> (Å) | <i>I</i> / <i>I</i> ₁ | <i>d</i> (Å) | <i>I</i> / <i>I</i> ₁ |
| 9.71 | 2 | 9.68 | 5 | | |
| 5.95 | 25 | | | 5.997 | 50 |
| 4.818 | 15 | 4.833 | 30 | | |
| 4.115 | 100 | 4.118 | 100 | | |
| 4.090 | 50 | | | 4.092 | 100 |
| 3.785 | 10 | 3.782 | 20 | | |
| 3.551 | 17 | 3.558 | 50 | | |
| 3.531 | 20 | | | 3.520 | 35 |
| 3.422 | 20 ^c | | | | |
| 3.366 | 15 | | | 3.358 | 32 |
| 3.230 | 25 | 3.228 | 45 | | |
| 3.160 | 3 | 3.155 | 3 | | |
| 3.022 | 27 | | | 2.994 | 36 |
| 2.910 | 15 ^c | | | | |
| 2.685 | 60 | 2.696 | 40 | 2.706 | 15 |
| 2.655 | 10 | | | 2.673 | 17 |
| 2.635 | 15 | 2.642 | 35 | | |
| 2.547 | 5 | 2.551 | 10 | | |
| 2.415 | 3 | | | 2.429 | 5 |
| 2.290 | 3 | 2.308 | 3 | | |
| 2.083 | 35 | 2.060 | 60 | | |
| 1.992 | 4 | | | 1.996 | 7 |
| 1.924 | 15 | 1.932 | 20 | 1.930 | 5 |
| 1.886 | 5 | 1.890 | 10 | | |
| 1.826 | 3 | | | 1.823 | 5 |
| 1.548 | 2 | | | 1.551 | 4 |

^a Filtered Cu $K\alpha$ radiation. d = interplanar spacing.

^b I/I_1 = relative peak intensity.

^c Broad peaks, not identified.

A Perkin-Elmer Process Vapor Fractometer, Model No. 184, was used to measure the concentrations of CO and CO₂ in the product stream. A molecular sieve column was used for CO and a column of 30% hexamethylphosphoramide on 60–80 mesh Fisher Columpak was used for CO₂. L and N Speedo-max recorders were used in conjunction with these instruments.

Analytical precision for the three measured compounds is about $\pm 2\%$ for each component. The IR and GPC instruments were calibrated daily with standard gas samples of known composition. The UV in-

strument was calibrated daily with an internal test screen.

The concentration of maleic anhydride was determined by the difference between the total carbon present in the benzene introduced and the total carbon present in the unreacted benzene, the CO, and the CO₂. The maleic anhydride concentration calculated from carbon balance difference agreed to within 2% with the values obtained by polarographic analyses of gas samples of the product stream. No benzoquinone nor phenol were detected.

Apparatus. A diagram of the reactor system is shown in Fig. 6. The carburetor containing benzene was maintained at $30 \pm 1^\circ\text{C}$ by means of a water bath. The glass reactor and preheat section was immersed in a lead-tin alloy bath whose temperature was controlled to $\pm 1^\circ$ by means of appropriate electronic relays. The bath temperature and the temperature inside the catalyst bed were detected by chromel-alumel thermocouples.

The reactor chamber contained 50 ml (48 g) of coated pellets supported on a small coil of nichrome wire. The temperature difference between the bed and the bath was found to increase with increasing extent of reaction only beyond 75% conversion of benzene. The catalyst void volume of 25 ml was measured by mercury displacement and the contact time is defined as the catalyst void volume divided by the flow rate in milliliters per second under standard conditions. The contact time was varied by changing the flow rate.

Procedure. Air was passed through the catalyst bed for 30 to 60 min prior to introducing benzene. Readings were taken only after a steady state of operation had been attained. Experiments were conducted at different initial concentrations of benzene, contact time, and temperature. The stability of the catalyst was assured by reproducing results obtained under particular conditions after 2 weeks of operation under varied conditions. Blank experiments using uncoated pellets demonstrated that no reaction occurred without the vanadium-molybdena catalyst up to 420°C .

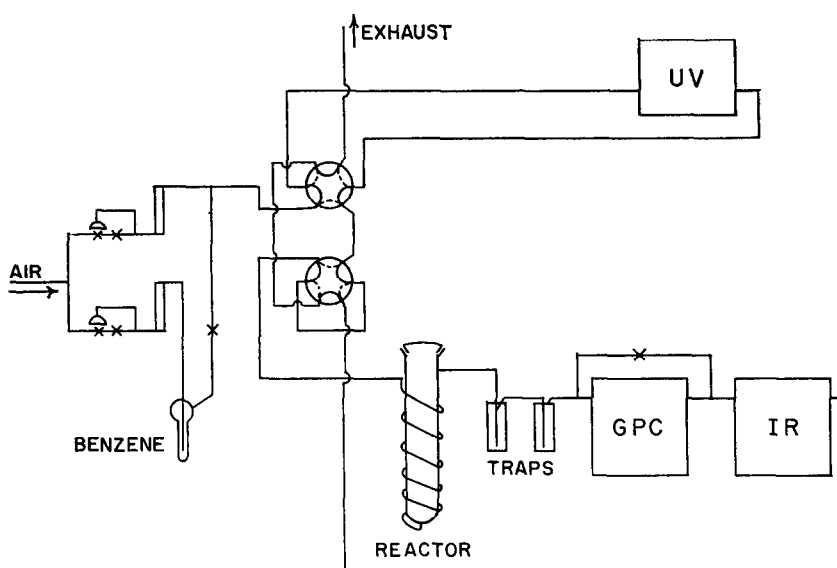


Fig. 6. Schematic diagram of the reactor.

REFERENCES

1. For reviews see (a) DIXON, J. K., AND LONGFIELD, J. E., in "Catalysis" (P. H. Emmett, ed.), Vol. 7, Chap. 3. Reinhold, New York, 1960; (b) MARGOLIS, L. YA., *Advan. Catalysis* **14**, 420 (1963).
2. BUTLER, J. D., AND WESTON, B. G., *J. Catalysis* **2**, 8 (1963).
3. IOFFE, I. I., AND LYUBARSKII, A. G., *Kinetics Catalysis (USSR) (Engl. Transl.)* **3**, 223 (1962).
4. BRETTON, R. H., WAN, S. U., AND DODGE, B. F., *Ind. Eng. Chem.* **44**, 594 (1952).
5. PETCHERSKAYA, Y. I., KAZANSKII, V. B., AND VOEVODSKY, V. V., *Actes Congr. Intern. Catalyse, 2^e, Paris, 1960*, **2**, 2121 (Éditions Technip, Paris, 1961).
6. KAZANSKII, V. B., EZHKOVA, Z. I., LYUBARSKII, A. G., VOEVODSKY, V. V., AND IOFFE, I. I., *Kinetics Catalysis (USSR) (Engl. Transl.)* **2**, 862 (1961).
7. IOFFE, I. I., EZHKOVA, Z. I., AND LYUBARSKII, A. G., *Russ. J. Phys. Chem. (Engl. Transl.)* **35**, 1160 (1961).
8. RAGLE, J. L., *J. Chem. Phys.* **38**, 2020 (1963).
9. HIROTA, K., AND KUWATA, K., *Bull. Chem. Soc. Japan* **36**, 229 (1963).
10. WEISS, J. M., AND DOWNS, C. R., *Ind. Eng. Chem.* **12**, 228 (1920).
11. HUGHES, M. F., AND ADAMS, R. T., *J. Phys. Chem.* **64**, 781 (1960).
12. ROITER, V. A., AND YUZA, V. A., *Kinetics Catalysis (USSR) (Engl. Transl.)* **3**, 343 (1962).
13. ROITER, V. A., *Actes Congr. Intern. Catalyse, 2^e, Paris, 1960*, **759** (Éditions Technip, Paris, 1961).
14. BOND, G. C., "Catalysis by Metals." Academic Press, New York, 1962.
15. STONE, F. S., *Advan. Catalysis* **13**, 1 (1962).
16. CAMERON, W. C., FARKAS, A., AND LITZ, L. M., *J. Phys. Chem.* **57**, 229 (1953).
17. D'ALESSANDRO, A. F., AND FARKAS, A., *J. Colloid Sci.* **11**, 653 (1956).
18. CALDERBANK, P. H., *J. Appl. Chem.* **2**, 482 (1953).
19. DUCHENE, J., AND LEPAGE, M., *Actes Congr. Intern. Catalyse, 2^e, Paris, 1960*, **2**, 2671 (Éditions Technip, Paris, 1961).
20. FABUSS, B. M., *Actes Congr. Intern. Catalyse, 2^e, Paris, 1960*, **2**, 2561 (Éditions Technip, Paris, 1961).
21. BUTLER, J. D., *Trans. Faraday Soc.* **56**, 1842 (1960).
22. HAYASHI, R., HUDGINS, R. R., AND GRAYDON, W. F., *Can. J. Chem. Eng.* **41**, 220 (1963).
23. BENSON, S. W., "The Foundations of Chemical Kinetics," p. 35. McGraw-Hill, New York, 1960.
24. WHEELER, A., *Catalysis* **2**, 105 (1955).
25. WEISZ, P. B., AND PRATER, C. D., *Advan. Catalysis* **6**, 144 (1954).

26. SATTERFIELD, C. N., AND SHERWOOD, T. K., "The Role of Diffusion in Catalysis." Addison-Wesley, Reading, Mass., 1963.
27. GLASSTONE, S., LAIDLER, K. J., AND EYRING, H., "The Theory of Rate Processes." McGraw-Hill, New York, 1941.
28. PARLIN, R. B., WALLENSTEIN, M. B., ZWOLINSKI, B. J., AND EYRING, H., in "Catalysis" (P. H. Emmett, ed.), Vol. 2, Chap. 5. Reinhold, New York, 1955.
29. SCHOLTEN, J. J. F., ZWIETERING, P., KONVALINKA, J. A., AND DE BOER, J. H., *Trans. Faraday Soc.* **55**, 2166 (1959).
30. ASTON, J. G., TOMESKO, E. S. J., AND FISHER, R. A., JR., *J. Am. Chem. Soc.* **86**, 2097 (1964).
31. KEMBALL, C., *Proc. Roy. Soc. (London)* **A187**, 73 (1946).
32. GREGG, S. J., AND WHEATLEY, K. H., *Proc. Intern. Congr. Surface Activity, 2nd, London, 1957* **2**, 102 (Butterworths, London, 1957).
33. SCHREINER, G. D. L., AND KEMBALL, C., *Trans. Faraday Soc.* **49**, 292 (1953).
34. BOOCOCK, G., AND CVETANOVIC, R. J., *Can. J. Chem.* **39**, 2436 (1961).
35. WHELAND, G. W., "Resonance in Organic Chemistry," p. 80. Wiley, New York, 1955.
36. SHELSTAD, K. A., Ph.D. Dissertation, Univ. of Toronto, 1958.
37. DOWNIE, J., Ph.D. Dissertation, Univ. of Toronto, 1959.
38. KAUZMANN, W., "Quantum Chemistry," p. 404. Academic Press, New York, 1957.
39. BRAND, J. C. D., AND WILLIAMSON, D. G., *Advan. Phys. Org. Chem.* **1**, 413 (1963).
40. The procedure followed is similar to that described in U. S. Patent 2,967,185 (January 3, 1961) [*Chem. Abstr.* **55**, 9727b (1961)].
41. NOUYRIGAT, F., *Bull. Soc. Chim. France*, p. 781 (1958).
42. MUNCH, R. H., AND PIERRON, E. D., *J. Catalysis* **3**, 406 (1964).